Available online at www.sciencedirect.com

SCIENCE DIRECT®

Polymer 47 (2006) 5239–5242

polymer

www.elsevier.com/locate/polymer

Polymer Communication

Morphology evolution in superheated crystal monolayer of low molecular weight poly(ethylene oxide) on mica surface

Dun-Shen Zhu [a], Yi-Xin Liu [a], An-Chang Shi [b], Er-Qiang Chen [a,*]

[a] *Department of Polymer Science and Engineering, and The Key Laboratory of Polymer Chemistry and Physics of Ministry of Education,*
College of Chemistry and Molecular Engineering, Peking University, Beijing 100871, China
[b] *Department of Physics and Astronomy, McMaster University, Hamilton, Ontario, 85 4M1, Canada*

Received 3 May 2006; received in revised form 5 May 2006; accepted 8 May 2006
Available online 19 June 2006

Abstract

Using atomic force microscopy (AFM) coupled with a hot stage, we studied the morphological evolution of superheated poly(ethylene oxide) (PEO) crystal monolayer on the mica surface. The PEO possesses a number average molecular weight (M_n) of 4250 g/mol and a polydispersity of 1.03. The superheated monolayer was obtained when the entire periphery of a triply-folded chain crystal [IF(3)] was thickened to be a twice-folded chain crystal [IF(2)] 'dam'. The IF(3) crystal was laterally confined by the IF(2) 'dam' and remained unchanged at its unconfined melting temperature (T_m). In superheated conditions, the interior IF(3) crystal unfolded, resulting in domains with a thickness in between the fold lengths of the IF(3) and the IF(2) crystals accompanied by hole formation. After its nucleation, the hole enlarged its area quickly and migrated long distances within the area bounded by the IF(2) crystal 'dam'.

Keywords: Superheated crystal; Monolayer; Poly(ethylene oxide)

1. Introduction

Both the crystallization and melting of polymers are thermodynamic first-order transitions. For polymer crystallization with a small supercooling, the melt may stay as a metastable liquid for a long time, because the free energy barrier of primary nucleation is high [1,2]. Therefore, a sufficiently large supercooling needs to be applied to promote the polymer crystallization process. By contrast, the free energy barrier for polymer crystal melting is usually shallow, and thus the superheating required is minimal. Conventionally, the observations concerning superheated phenomenon of polymer crystals are related to the heating rate effect where the crystals are heated faster than their thermal conductivity [3]. The first case of genuine isothermal superheating was reported by Kovacs et al. [4]. Using a poly(ethylene oxide) (PEO) fraction with a number average molecular weight (M_n) of 6000 g/mol, they grew the twice-folded chain single crystals [IF(2)] followed by the once-folded chain crystals [IF(1)]. The resultant lamellar crystals were composed of the IF(2) crystal bounded around the edges by the IF(1) crystal. At temperatures higher than the IF(2) melting point [$T_m(2)$], the unstable crystal interior remained unaffected for fairly long periods of time. Another example was observed in the single crystals of syndiotactic polypropylene (st-PP) grown from thin film melt that exhibited two sectors with different thicknesses [5,6]. The st-PP crystal in the thinner (010) sectors possesses a melting temperature (T_m) lower than that in the thicker (100) sectors. It was observed that the melting of the (010) sector could stop as soon as thicker crystals formed along the crystal/melting boundaries via recrystallization/reorganization. The just developed thicker lamellae created 'dams' to confine the rest (010) sectors in a two-dimensional space [6].

In this communication, we report our experimental observations on the superheated PEO crystal monolayer on the mica surface. It is known that the low molecular weight (LMW) PEO fractions can form flat-on monolayer lamellae on the hydrophilic substrates [7–11]. Being identical to the LMW PEO lamellae formed in the bulk [4,12–16], the monolayers are integral folding chain crystals [IF(n)], of which the fold number n is supercooling dependent. Using a crystallization procedure similar to that utilized by Kovacs described in [4], we were able to obtain a composite monolayer of LMW PEO with an IF(3) crystal interior confined by IF(2) crystal at the

---

* Corresponding author. Tel./fax: +86 10 6275 3370.
E-mail address: eqchen@pku.edu.cn (E.-Q. Chen).

0032-3861/$ - see front matter © 2006 Elsevier Ltd. All rights reserved.
doi:10.1016/j.polymer.2006.05.013

periphery on the mica surface. The morphological evolution of the superheated IF(3) crystal was investigated by in situ atomic force microscopy (AFM) coupled with a hot stage.

2. Experimental section

The LMW PEO fraction (HPEO4250) with both the chain end groups of –OH was purchased from Polymer Laboratories, Ltd, of which the M_n is 4250 g/mol and the polydispersity is 1.03. The ultrathin films of HPEO4250 on the freshly cleaved mica surfaces were prepared by static solution casting method. Typically, a drop (∼40 μl) of the HPEO4250/methylene chloride solution with a concentration of 5×10^{-4} g/ml was pipetted onto the substrate at around 25 °C; the excess solution was blotted by filter paper. The samples were dried under ambient conditions and later in vacuum for several days. After being melted at 70 °C, the samples were quenched to a crystallization temperature (T_c) below 30 °C.

An AFM (DI NanoScope IIIa) coupled with a hot stage was utilized to examine the morphology of the HPEO4250 samples after crystallization, during heating and annealing. The temperature of the AFM hot stage was calibrated using standard materials to have an accuracy of ±0.2 °C. The height and phase images of the lamellar crystals were recorded using taping mode AFM, wherein the cantilever force was controlled to be large enough to explore the surface features, yet small enough to avoid the sample damage. The AFM images were recorded at a scan rate of 1 Hz with a resolution of 256×256. Therefore, the time required for every AFM image is ∼4.3 min.

3. Results and discussion

The as-cast HPEO4250 ultrathin films on the mica surface possessed a thickness of 6–7 nm with a finger-like morphology. At 70 °C, which is higher than the equilibrium T_m of HPEO4250, the crystals were completely melted. The PEO melt on the hydrophilic mica surface is pseudo-dewetting, wherein the PEO molecules directly adsorbed onto the substrate form a continuous thin wetting layer, and the rest of the material form droplets on the wetting layer [7,8]. While the isothermal crystallization from such a melt was found to be very difficult at a T_c above 30 °C, quenching to room temperature would readily lead to finger-like crystal monolayers (Fig. 1(a)). The resultant lamella had a measured thickness of 6.5 nm (see the inset of height profile in Fig. 1(a)), which is identical to the theoretical fold length of the HPEO4250 IF(3) crystal with the chains perpendicular to the substrate [4,9,11–16].

To investigate the melting behavior, we slowly heated the IF(3) crystal monolayer using our AFM coupled with the hot stage. Fig. 1 presents the AFM images of a HPEO4250 sample after crystallization at 25 °C (Fig. 1(a)) followed by annealing at 35 °C (Fig. 1(b) and (c)). During heating, the morphology of the original IF(3) crystal was stable below 35 °C. However, once the temperature reached 35 °C, the 'fingers' of the IF(3) crystal started to shrink their boundaries, which was recognized as a sign of melting. Meanwhile, thickened domains with a height of 9.0 nm appeared along the monolayer periphery (see the inset of height profile in Fig. 1(b)). This thickness is identical to the predicted height of the HPEO4250 IF(2) crystal monolayer. Therefore, we consider that the T_m of the IF(3) crystal [T_m(3)] is to be 35 °C, and the IF(3) crystal transforms into the IF(2) crystals, most likely, via melt/recrystallization [11,16]. While annealing at 35 °C, Fig. 1(b) at 30.1 min and Fig. 1(c) at 72.7 min evidence that the IF(3)→IF(2) transformation progresses continuously. This thickening process can completely break down the original IF(3) crystal monolayer (see the portions indicated by the ellipses in Fig. 1(c)). Compared to the IF(3) crystal, the newly formed IF(2) crystal covers less area. Nevertheless, also shown by Fig. 1(c) (see the area indicated by the square), when the entire perimeter of the 'fingers' got thickened to be IF(2) crystal, the interior IF(3) crystal is stable for a prolonged annealing time at 35 °C. In this case, the IF(2) crystal at the IF(3) crystal periphery functions like a close 'dam' that provides confinement fixing the interior PEO chains in a two-dimensional space.

It is intriguing to examine the confined superheated IF(3) crystal. Fig. 2 is a set of AFM images obtained at different times after the sample shown in the square of Fig. 1(c) was brought to an annealing temperature (T_a) of 39 °C, which is

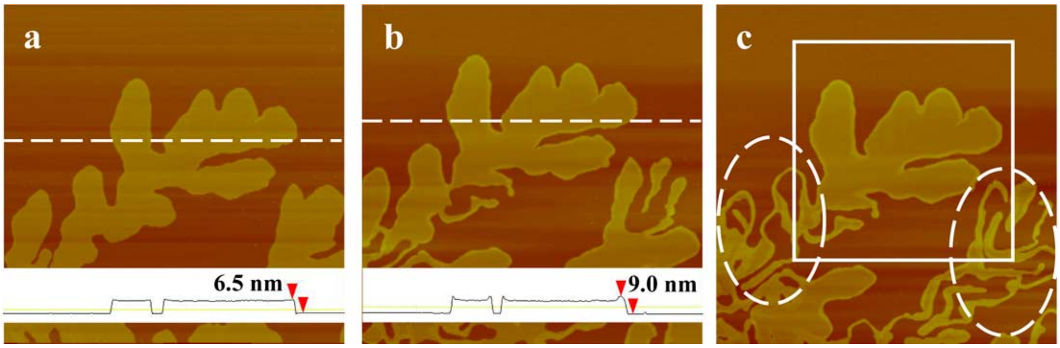

Fig. 1. A set of AFM high images of HPEO4250 after crystallization at 25 °C (a) followed by annealing at 35 °C ((b) and (c)). (b) and (c) were recorded at different annealing time of 30.1 and 72.7 min, respectively. The size of the images is 7×7 μm^2. The insets of (a) and (b) are the height profiles along the corresponding white dashed lines.

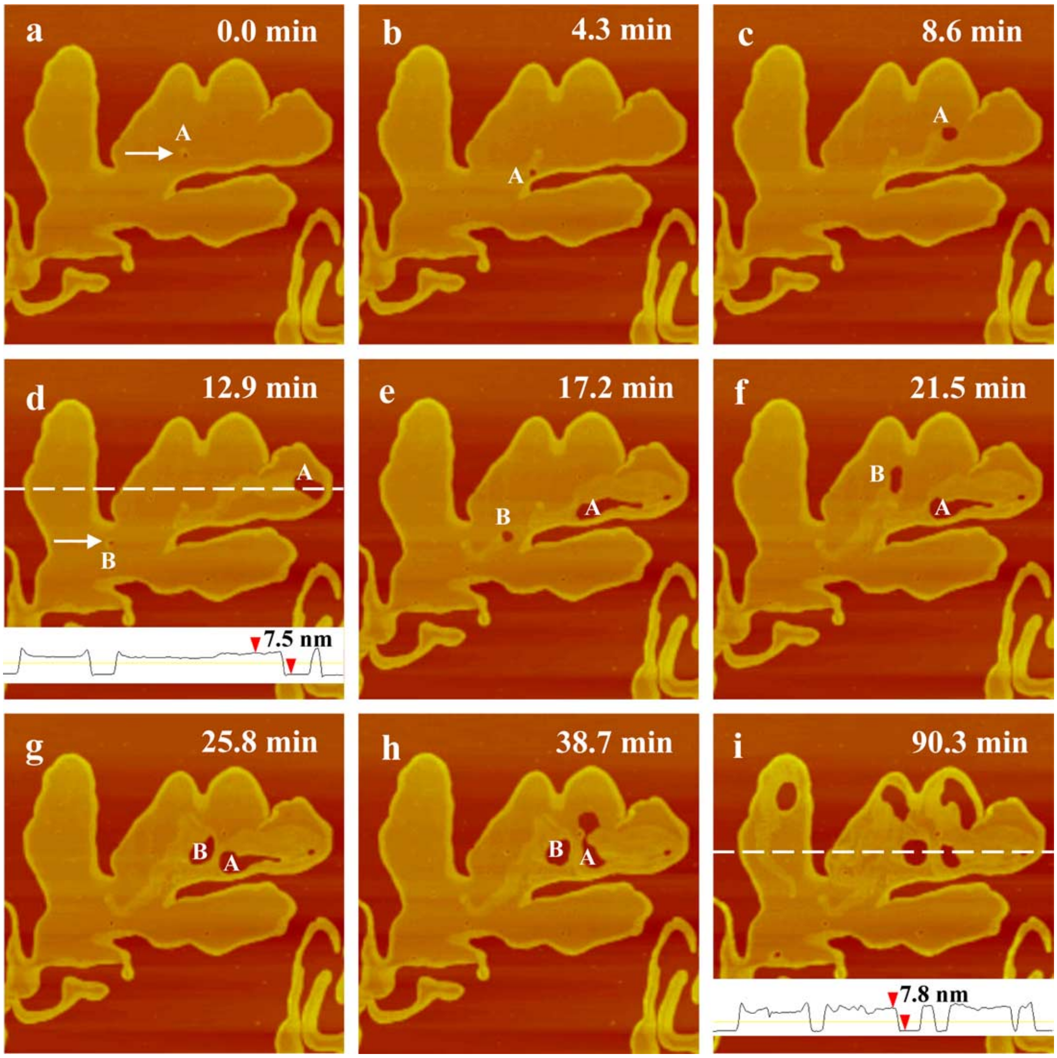

Fig. 2. A set of AFM height images obtained at 39 °C at different annealing time. The images were taken at the area indicated by the square in Fig. 1(c). The size of the images is $4.5\times4.5\ \mu\mathrm{m}^2$. The birthplaces of the holes A and B are pointed by the arrows in (a) and (d). The insets of (d) and (i) are the height profiles along the corresponding white dashed lines.

4 °C higher than the $T_{\mathrm{m}}(3)$ but 5 °C lower than the $T_{\mathrm{m}}(2)$. The $T_{\mathrm{m}}(2)$ of HPEO4250 was also determined with AFM using the same criterion as that mentioned above for $T_{\mathrm{m}}(3)$. From these images, we observe that the width of IF(2) crystal 'dam' formed at 35 °C is almost unchanged during the isothermal annealing, but in the area enclosed by the 'dam', a dramatic morphological evolution takes place. In the first image recorded at 39 °C (Fig. 2(a)), only one small hole (the hole A, pointed by the arrow) with a diameter of $\sim$55 nm is observed. It is conceivable that the IF(2) crystal 'dam' only confines the IF(3) crystal laterally in two-dimensions, but allow the PEO chain to slide along the crystalline *c*-axis perpendicular to the mica surface. As the vertical chain sliding motion enables larger fold lengths, the superheated IF(3) crystal increases its thickness and thus decreases its free energy. This process is accompanied by the creation of lattice vacancies. Therefore, the halo observed in Fig. 2(a) could be attributed to the merging of the lattice vacancies.

Fig. 2(a)–(g) are the successive AFM images with a time interval of 4.3 min. Strikingly, we observe that the hole can not only enlarge its size, but can also explore the area within the IF(2) crystal 'dam'. For instance, the hole observed in Fig. 2(a) grows in size and moves closer to the 'dam' as seen in Fig. 2(b). The distance between the two holes in Fig. 2(a) and (b) is $\sim$300 nm. In Fig. 2(c), the hole's center is even $\sim$1 μm away from that in Fig. 2(b). The trajectory of the hole moving can be traced by a 'tail', which is in fact a thickened domain with a height of 7–8 nm (see the insets of the height profiles along the dashed lines in Fig. 2(d) and (i)). For a later developed hole (the hole B in Fig. 2), the same behavior of hole growth and migration can also be observed. Fig. 2(h) and (i) illustrate that the more holes are created, and the motion of holes gradually slows down and eventually stops as they are surrounded by the thickened areas.

As suggested above, the PEO chain sliding motion along the crystalline *c*-axis is active when the IF(3) crystal enters its superheated state, which will lead to the PEO chain unfolding. In our experiment, we note that instead of forming the IF(2) crystals, the thickened domains within the IF(2) crystal 'dam' possess the thickness of 7–8 nm, and thus, the HPEO4250 chains therein are in a transient non-integral folding (NIF) state. Yet this phenomenon could not be observed during isothermal crystallization nor melt/recrystallization experiments with HPEO4250 on the mica surface. Therefore, the existence of a NIF crystal with a considerable long lifetime may be attributed to the lateral confinement arising from the IF(2) crystal 'dam'.

From the perspective of mass conservation, the unfolding of the superheated IF(3) crystal is naturally related to forming the lattice vacancies (the holes). The creation of a new hole is a slow nucleation process. As shown in Fig. 2, the incubation time of the hole B is apparently ~12 min. However, once a hole is created, the hole growth and migration are rather fast. This should be due to a fast chain lateral motion. When the hole moves to different locations, the previously empty space has to be refilled by the PEO chains. The height profiles shown in the insets of Fig. 2(d) and (i) illustrate that the bottom of the hole is at the same level as the mica surface outside the IF(2) crystal 'dam'. This indicates that no molten PEO chains adsorbed onto the mica substrate within the hole to form a wetting layer. We suspect that the hole refilling is not a classical melt/recrystallization process. The PEO chains moving towards the previous hole location might mainly take place along the perimeter of the hole. The mechanism underlying can be that the chains on the hole surface keep their registration in the crystalline lattice, and thus move via a cooperative sliding motion. Alternatively, the chains on the hole surface could be already melted, and they diffuse to new positions to pack into the crystalline lattices again, behaving similar to the chains adsorbed on the crystal growth front in melt crystallization. Further investigations are necessary to understand this interesting annealing process.

4. Conclusion

In summary, we have investigated the morphological evolution of the superheated LMW PEO crystal monolayer on the mica surface. While the entire periphery of a HPEO4250 IF(3) crystal monolayer was thickened to form a close 'dam' of IF(2) crystal, the confinement imposed by the 'dam' made the interior IF(3) crystal remain at its T_{m}. The chain unfolding of the superheated IF(3) crystal resulted in thickened domains with a height in between the fold lengths of the IF(3) and the IF(2) crystals, which was accompanied by the hole formation. The hole enlarged its size quickly once it was created within the superheated IF(3) crystal. Moreover, the hole could migrate long distances, leaving a thickened 'tail' behind it. The detailed analysis of the kinetics and thermodynamics of the hole formation and growth within the superheated monolayer is currently being undertaken in our laboratory.

Acknowledgements

This work was supported by the National Natural Science Foundation of China (Grant no. 20234020, no. 20025414, and no. 20374003).

References

[1] Keller A, Cheng SZD. Polymer 1998;39:4461.
[2] Cheng SZD, Keller A. Ann Rev Mater Sci 1998;28:533.
[3] Wunderlich B. Thermal analysis. Boston: Academic Press; 1990.
[4] Kovacs AJ, Straupe C, Gonthier A. J Polym Sci, Polym Symp 1977;59:31.
[5] Bu Z, Yoon Y, Ho RM, Zhou W, Jangchud I, Eby RK, et al. Macromolecules 1996;29:6575.
[6] Zhou W, Cheng SZD, Putthanarat S, Eby RK, Reneker DH, Lotz B, et al. Macromolecules 2000;33:6861.
[7] Reiter G, Sommer JU. Phys Rev Lett 1998;80:3771.
[8] Reiter G, Sommer JU. J Chem Phys 2000;112:4376.
[9] Reiter G, Castelein G, Sommer JU. Phys Rev Lett 2001;86:5916.
[10] Schonherr H, Frank CW. Macromolecules 2003;36:1188.
[11] Zhai XM, Wang W, Ma ZP, Wen XJ, Yuan F, Tang XF, et al. Macromolecules 2005;38:1717.
[12] Buckley CP, Kovcas AJ. In: Hall IH, editor. Structure of crystalline polymers. New York: Elsevier; 1984. p. 261–307.
[13] Cheng SZD, Zhang AQ, Barley JS, Chen JH, Habenschuss A, Zschack PR. Macromolecules 1991;24:3937.
[14] Cheng SZD, Chen JH, Zhang AQ, Barley JS, Habenschuss A, Zschack PR. Polymer 1992;33:1140.
[15] Cheng SZD, Chen JH, Barley JS, Zhang AQ, Habenschuss A, Zschack PR. Macromolecules 1992;25:1453.
[16] Chen EQ, Jing AJ, Weng X, Huang P, Lee SW, Cheng SZD, et al. Polymer 2003;44:6051.